NATIONAL RADIO ASTRONOMY OBSERVATORY
Green Bank, West Virginia

DESIGN CONSIDERATIONS FOR THE NRAO INTEFEROMETER

By

NIGEL J. KEEN

AUGUST 1963

DESIGN CONSIDERATIONS FOR THE NRAO INTERFEROMETER

I. Abstract

The NRAO interferometer project is discussed and the reasons for choice of equipment and operating parameters (e.g., bandwidth, central IF, LO frequency) are given. The double sideband interferometer system used at Cal. Tech. [1] will be employed, with parametric RF amplifiers preceding the crystal mixers. The LO frequency will be 2695 Mc at the center of a 20 Mc RF bandwidth. A block schematic diagram is shown in Figures I(a) and I(b).

II. The Interferometer Baseline

The choice of baseline was limited by geographical considerations once a high resolution interferometer was required. The baseline azimuth is 243° with respect to the present 85-foot dish, and the second 85-foot dish is to have sites along this baseline at 1200, 1500, 1800, 2100, 2400, and 2700 meters from the existing dish. Hence, Fourier components will be obtained in the middle of those of Jodrell Bank at 158 Mc (61,000 λ, 32,000 λ, 9700 λ, and 2200 λ) [2] and above these of Cal. Tech. at 960 Mc [1] [3] and Meudon at 1420 Mc [4] (baselines up to 1600 λ and 7000 λ, respectively). The baseline azimuth chosen at NRAO will produce the variation of fringe frequency with hour-angle shown in Figure II.

A baseline azimuth rotated from the E-W direction gives an increased variation of projected baseline rotation (on the celestial sphere); the projected baseline rotation for the NRAO interferometer is shown in Figure III. According to Rowson [5], the increased variation due to the skewed baseline gives more information on sources, although no quantitative assessment has been made. This would depend to a large extent on the source models assumed, since the same number of points on the u-v diagram are determined for any baseline azimuth.

III. The Receiver System

The schematic diagram is shown in Figure I. The basic system employed by Cal. Tech. [1] is to be used for the NRAO interferometer, and, in addition, parametric amplifiers will be inserted in front of each mixer. These should reduce the system

temperature from $\sim$ 900 °K to $\sim$ 150 °K [6]. Although parametric amplifiers without cooling may now have noise temperatures of around 80 °K [7], cable losses and the contribution from the IF mixer will add as much as 70 °K.

Apart from the practical difficulties in correlating wide-band signals, parametric amplifiers have a maximum gain-bandwidth product of around 500 Mc at present [7], so that a 20 Mc bandwidth is a reasonable compromise: keeping the IF noise contribution down while giving a reasonable bandwidth. It may be seen (Figure IV) that excessive reduction of the bandwidth below 20 Mc would accentuate the effect of the "gap" in the double sideband signal passed through a 2-10 Mc IF amplifier. Reducing the bandwidth of either parametric amplifier or IF amplifier increases the fraction of pass-band wasted.

IV. Processing the IF Signals

(a) General.

After passing through IF amplifiers the two signals are multiplied and integrated. If we assume a time lag τ between times of signal arrival we have an integrator output

$$\int_{-\infty}^{\infty} X(t)\, X(t - \tau)dt$$

for extremely long integrating times. This is the cross-correlation of the two signals [8].

According to the calculations of Read [1] the interferometer fringes are amplitude modulated by IF fringes, the number of RF fringes in one cosinusoidal "envelope" being $\frac{f_{LO}}{2f_{IF_o}}$. Furthermore, a finite gaussian bandpass gives a further gaussian modulation, the half-width of this modulation being inversely proportional to the square of the bandwidth (see Figure V). This modulation is of the form $\frac{\sin X}{X}$ for a rectangular pass-band. The position of the maximum of one of the cosinusoidal envelopes and the maximum of the band-pass function may be moved simultaneously by adjusting the relative IF delay: in the double-sideband interferometer the central RF fringe is defined only by the position of this maximum. The number of RF fringes experiencing less than a p percent amplitude reduction due to both envelope and bandpass functions is shown in Figure VI.

Since λ_{IF_o} = 50 m, it would appear — from the effect of bandpass function on RF fringe amplitude (Figure VII) — that the exponential passband would reduce RF fringe amplitudes in the envelope adjacent to the zero-delay envelope by 5 percent, while the

rectangular passband reduces interferometer fringe amplitudes by about half that amount. Thus, only the central IF envelope would be used. (It should be remembered that a gaussian passband gives an unreal situation for $\frac{\Delta f}{f} \longrightarrow 1$, since much of the bandpass occurs in the negative frequency region.)

One interesting point that arises from Figures VI and VII is the negligible effect of a bandpass of the same order as f_{IF_o} on the interferometer fringes in the central envelope.

A more general method of obtaining the fringe modulation is to consider the two "white" noise voltages passing immediately through rectangular IF passbands, being multiplied together and the result being integrated. This is justified for a (virtually) monochromatic LO signal, as is shown by Burns [9] and Wagner [10], and considered in Appendix I.

(b) Multiplication and Integration Considerations.

We have assumed ideal integration of the multiplied signals, i.e., no charge leakage from the capacitor of the RC integrator. Such an integration is in fact obtained using a voltage-to-frequency converter, where the voltage is integrated and "dumped" over each sampling interval. It may be shown [11] that cross-correlating (sampling) a periodic signal embedded in noise with pulses of the same period gives a signal-to-noise ratio gain of $\sqrt{\text{number of samples}}$. This assumes integration prior to sampling, so that this is not a true sampling technique. The method is considered in Appendix II.

Since the above method would require a large number of samples per fringe-cycle for an integral number of samples to give a reasonably small error, and since the cycle period is not constant, a method of greater flexibility and accuracy is described in Appendix IV. The computer processing of the data is also outlined.

(c) A Direct Correlation System.

A method of correlating the signals entirely by digital methods would be to heterodyne the IF signal from each antenna down to video frequencies, and to pass the video signals through a (sharp cut-off) low-pass filter prior to clipping. This procedure is similar to that of Weinreb [12]. The two filtered and clipped signals are now sampled at a rate 2B, and corresponding points on each sample multiplied together. The products are

then added over a discrete fraction of a fringe period (for a given number of sample products, n). This gives a point on the digital fringe pattern. The process is repeated for the next n sample products, and so on. Thus, the fringe pattern will be digitally reconstituted if the sample products are added over times small compared to the fringe period but large compared to the sampling interval. Since we are now considering digital signals, the problems of amplification and transmission are a standard communications technique. There only remains the problem of synchronizing the two "records". The delay in receiving the digital record from the "distant" antenna presents no problem if there are facilities for storing the digital record from the "home" antenna until the "distant" pulses arrive. Since phase information is now at video frequencies, fluctuations in the sampling period may be permitted, provided they are small compared with the highest video period. The problem of LO phase stability still remains, however.

One of the difficulties in the use of clipped noise appears to be the retention of absolute fringe amplitude information. The practical realization of a cross-correlator will anyhow be considered at a later date.

(d) The Multiplier.

The multiplication of RF signals presents considerable technical problems, so multiplication of IF signals is used. Even here the signal bandwidth presents problems. It is proposed to use the Cal. Tech. multiplier, modified for the higher $\frac{\Delta f}{f_{IF_o}}$ at NRAO. Experiments on the multiplier are now in progress.

(e) The Integrator and Recorder.

Interferometer fringes will be complied digitally, although an RC and recorder give an analog record as an instrumental check. The output of the multiplier will be passed to a voltage-to-frequency converter, and an integrated record obtained over the (constant) integrating interval. In choosing the integrating interval, the accuracy with which the fastest fringe may be computed must be considered in terms of the minimum number of points required. The method of obtaining a sine wave from a constant observation rate on a sine wave of varying frequency is considered in Appendix IV. The determination (and accuracy) of the phase and amplitude of this sine wave is considered in

Appendix V. We consider the number of digits required for a reasonably accurate record of the smallest fringe amplitude in Appendix VI.

V. The Phase-Lock Loop

The relative phase of the LO signals arriving at the mixers at each antenna must be constant. Thus, a phase locking system is required, such as the system used by Cal. Tech. [1]. It is hoped that the Cal. Tech. system will prove adequate for the NRAO interferometer, although field tests will have to be performed in view of the longer baseline and the higher LO frequency. The block schematic is shown in Figure I(b). A possible disadvantage of this system is the variation of electrical path from the HF reference to one antenna only. An alternative system is shown in Figure I(c).

VI. The Problem of Absolute Phase

The accurate location of sources requires the location of the central fringe for every observation. This has been achieved [1] by using calibration sources in the region of the observed source, although the much higher fringe frequencies to be employed at NRAO require correspondingly greater accuracy in delay calibrations. The problem of the phase stability of the fringes is under consideration at the moment.

VII. Observations and Data Reduction

(a) The Data.

The output of the interferometer will be a series of digital readings on tape, taken at fixed intervals (in sidereal time). Each scan will commence with date, sidereal time, a program number, declination and right ascension of individual antennas, and relevant delay settings. The sampling rate is determined by calculating the minimum number of samples per cycle of a "noisy" sine wave to give rms amplitude and phase errors of less than p percent. The maximum fringe frequency is 1.5 cycles per second (see Appendix V).

Neglecting the change in fringe frequency with time, a one-minute interferometer scan gives a maximum least-squares error of 8 percent between -5 HA and +3 HA for $\delta = 0°$ (see Appendix III). In fact, the assumption of constant frequency fringes will usually

give considerably smaller errors. If this frequency-shifting is not tolerable, a scheme such as that outlined in Appendix IV may be used. This scheme is more flexible than the assumption of fixed frequency, and the length of the interferometer scan here is limited only by the "smearing" of the observation point on the u-v plane. The method of least-squares fit is used to determine the phase and amplitude of the sine wave. The method is shown in Appendix V.

For a bandwidth of 8 Mc, and a scan time of 50 seconds (assumed to be the integration time), a crystal mixer gives an rms noise temperature of 0.05 K. Hence, according to the criterion of von Hoerner [13] the smallest measurable flux density using the crystal mixer alone is

$$S_{min} = \frac{2kT_o q_n}{2A\sqrt{B\tau}}$$

$$\simeq 0.6 \text{ flux units}$$

for a two antenna interferometer. The system noise temperature (T_s) is taken as 1000 K (the parametric amplifier gives $S_{min} \simeq 0.08$ flux units). Also, the number of observable sources per steradian should be $\sim$ 250. For a fifty percent sky coverage this gives $\sim$ 1500 observable sources, which includes at least nine point sources [14] (unresolved at 32,000 λ [2]). The method of von Hoerner should be used with caution, however, when considering the interferometer. In fact, integration is only over parts of the fringe cycle, so S_{min} is increased by $\sqrt{n}$, where n is the number of points taken per cycle (see Appendix V). This still leaves us nine point sources for n = 10, with $\sim$ 100 sources per steradian (see Appendix VII).

Since the path through the atmosphere is longer at low elevations, the phase fluctuations may increase considerably. Let r be the length through the atmosphere, and let Δr be the differential path for the two beams. Assuming $\Delta r \sim r^{\alpha}$, where $0 < \alpha < 1$, then $\Delta r \sim \frac{h}{\cos \Theta}^{\alpha}$

where h = height of atmosphere (assumed constant)
and Θ = angle to the zenith.

Also $x = D \sin \Theta$

where D = geographical baseline,
and x = path difference.

Hence $\Delta x = D \cos \Theta \, \Delta\Theta$, and since $\Delta x \sim \Delta r$

$$\Delta\Theta \sim \frac{1}{D(\cos \Theta)^{1+\alpha}}$$

Since large values of Θ give closer beams, the uncorrelated path fluctuations may decrease to some extent. Anyhow, the above hypothesis will have to be tested experimentally.

The scales of Figures II and VIII are the same, so we see that the NRAO interferometer could not be very useful for studying Cygnus A with existing system noise temperatures ($\sim$ 1000 °K). A standard computer program now exists at NRAO to give phase and amplitude contours of any double gaussian source, provided the following information is given:

i. Position angle,
ii. Gaussian half-widths (assumed equal),
iii. Component separation,
iv. Ratio of component intensities,
v. Extent and intervals of u-v plane, and
vi. Contour intervals.

VIII. Conclusions

The system described for the NRAO interferometer is essentially similar to that of Cal. Tech., although more rigorous stability specifications are required due to the higher operating frequency and the longer baselines.

Some modifications will be incorporated at a later date, since the interferometer is to be both an observing instrument and a test bench. It is probable that phase and delay stabilities will present problems in the early stages of operation. Thus, we intend to avoid the use of the parametric amplifiers and digital read-out until the stability of the actual interferometer system has been checked.

APPENDIX I

THE CORRELATION OF TWO RANDOM GAUSSIAN SIGNALS

Consider the multiplication of two white stationary noise voltages after each has passed through a rectangular IF passband. The noise voltages will have the characteristic $\frac{\sin \omega_1 t}{\omega_1 t}$ form. The correlation of the two signals gives the function (unintegrable in closed form)

$$f(\tau) = \int_{-\infty}^{\infty} \frac{\sin \omega_1 t}{\omega_1 t} \cdot \frac{\sin \omega_1 (t - \tau)}{\omega_1 (t - \tau)} dt$$

This will give the fringe modulation envelope pattern if the limits of integration are times large compared with τ. The term describing the actual RF fringes has been neglected here.

We see that $f(\tau)$ is the convolution

$$f(\tau) = q(t) \ast q(t - \tau)$$

where the Fourier transformation is given by

$$F(\omega) = [G(\omega)]^2$$

$$= \text{constant where } \omega_1 < \omega < \omega_2, \text{ and zero outside}$$

Let the constant be unity, i.e.,

$$f(\tau) = \int_{\omega_1}^{\omega_2} \cos \omega\tau \, . \, d\omega \qquad (1)$$

$$= \frac{1}{\tau} [\sin \omega_2 \tau - \sin \omega_1 \tau]$$

$$= \frac{2}{\tau} \sin \left(\frac{\omega_2 - \omega_1}{2} \right) \tau \cos \left(\frac{\omega_2 + \omega_1}{2} \right) \tau$$

$$= B \frac{\sin \frac{B\tau}{2}}{B\frac{\tau}{2}} \cdot \cos \omega_{IF_o} \tau \qquad (2)$$

This is the amplitude modulation of the RF fringes, i.e., the fringe envelope.

For a gaussian passband centered at IF_o equation (1) becomes

$$f(\tau) = \int_{-\infty}^{\infty} \left[e^{-\frac{\left(\omega - \omega_{IF_o}\right)^2}{2\sigma^2}} \right] \cdot \cos \omega\tau d\omega$$

From which it may be shown that

$$f(\tau) = \sigma\sqrt{2\pi} \cos \omega_{IF_o} \tau \cdot e^{-\frac{\sigma^2\tau^2}{2}}$$

$$= B\sqrt{\frac{\pi}{2}} \cos \omega_{IF_o} \tau \cdot e^{-\frac{B^2\tau^2}{8}} \qquad (3)$$

where we define $B = 2\sigma \simeq$ gaussian half-power bandwidth.

From either (2) or (3), $B \longrightarrow 0$ gives the Cal. Tech. result [1].

APPENDIX II

PERIODIC SAMPLING OF A WAVE OF KNOWN FREQUENCY

If n is the sampling rate and N is the number of samples per cycle (the period being obtained from a table or computer program), samples 1, N + 1, 2N + 1, 3N + 1 ... are added together to give the first point on the fringe pattern. The process is repeated, starting with the second sample, and adding samples N + 2, 2N + 2, 3N + 2 ... This gives the second point. The process is repeated until all samples have been used once. A ten-second interferometer record sampled every $\frac{1}{100}$ second has a signal-to-noise gain of $\sqrt{1000}$ over a single sample. By contrast, cross-correlation between the signal embedded in noise and the actual periodic signal (as opposed to samples) gives a signal-to-noise ratio gain of $\sqrt{500}$ from the same number of observations. The determination of n is considered in Appendix V, with special reference to fringe phase and amplitude errors.

An integrator with short a time constant (compared with the sampling interval) gives extremely inaccurate integration and does not smooth out the higher frequency fluctuations effectively. A long time constant attenuates and disperses the signal, i.e., shifts phase of the fringes according to fringe frequency. Vinokur [16] has calculated that only a 2 percent loss of information occurs at each sampled point if the time constant, T, is twice the sampling period, Θ. This is effectively a reduction in signal-to-noise ratio of 2 percent. For $T = \Theta$ the error at each point is 8 percent. The sum of samples added together is the number of fringes in one scan of the source, and we see (Fig. III) that a one-minute scan time introduces a maximum fringe fluctuation of one percent between -5 H.A. and +3 H.A. This gives a maximum error of 3 percent in assuming constant frequency (see Appendix III). In the region of the instrumental meridian the fringe frequency is virtually constant, and a larger number of fringes per scan may be taken.

APPENDIX III

TO CALCULATE THE LEAST SQUARES ERROR IN FITTING A SINE WAVE OF CONSTANT FREQUENCY TO ONE OF VARIABLE FREQUENCY

$$\epsilon(\tau) = \frac{\int_0^T [\cos 2\pi f t - \cos 2\pi f t]^2 dt}{\int_0^T \cos^2 2\pi f t dt}$$

However, f = f(t) and this complicates calculations considerably. A good approximation is the method used below.

Each sine wave is experiencing a time shift and a frequency shift, relative to the reference (in this case, center) cycle. Let us consider the two shifts separately.

Considering the time shift, let us assume two sine waves of equal frequency (see Figure IX), every cycle of the second sine wave being displaced from the corresponding cycle of the first (reference) sine wave by an increasing time lag. Let T be this time lag. We consider the least squares fit for one cycle, the mean square error being

$$\epsilon = \frac{\int_0^2 [\cos \bar{\omega} t - \cos \bar{\omega}(t + T)]^2 dt}{\int_0^{2\pi} \cos^2 \bar{\omega} t dt}$$

$$= \frac{\int_0^{2\pi} [4 \sin^2 (t + \frac{T}{2}) \bar{\omega} \sin^2 \frac{T}{2} \bar{\omega}] dt}{\pi}$$

$$\boxed{\epsilon = 4 \sin^2 \frac{T}{2} \bar{\omega}}$$

This gives us the mean square error for two sine waves of equal frequency, offset by T.

Consider now the change in frequency (see Figure X). The lengths of individual cycles in Figure IX(b) are altered in order to give a continuous wave. The mean square error in this process is, for the smallest variations, one-half of that due to the time shifts, and decreases the total error. Thus, the mean square error due to both frequency and time shift $\simeq 0.5\,\epsilon$ per cycle.

We calculate the change in frequency per cycle, and the reference frequency from which this change occurs. From the graph of fringe frequency against time (Figure II),

the maximum gradient between - 5 HA and +3 HA is at $\delta = 0°$ where $f = 0.34$ and $\frac{df}{dt} = 4.5 \times 10^{-5}$. We are, of course, calculating the change of cycle period only to calculate time shifts.

The delay contribution of the n^{th} cycle

$$t_n = \frac{1}{f_n} - \frac{1}{\bar{f}}$$

$$T_n = t_1 + t_2 + \ldots + t_n$$

$$= \frac{1}{f_1} + \frac{1}{f_2} + \ldots + \frac{1}{f_n} - \frac{n}{\bar{f}}$$

$$f_n = \bar{f} - \frac{n}{\bar{f}} \frac{df}{dt} \ldots$$

$$T_n = \sum_{m=1}^{n} \frac{1}{\bar{f} - \frac{n}{\bar{f}} \frac{df}{dt}} - \frac{n}{\bar{f}}$$

$$= \sum_{m=1}^{n} \frac{1}{\bar{f}} \left(1 + \frac{n}{(\bar{f})^2} \frac{df}{dt}\right) - \frac{n}{\bar{f}}$$

since $\frac{n}{(\bar{f})^2} \frac{df}{dt} << 1$. For a one minute scan we have two identical half-minute scans, since the reference cycle is at the scan center. Hence, $n = 30 \times 0.34 \simeq 10$. Hence

$$T_{10} = \frac{1}{(\bar{f})^2} \cdot \frac{df}{dt} \sum_{m=1}^{10} m$$

$$= 3.9 \times 10^{-4} \sum_{m=1}^{10} m$$

Now $$\epsilon = 4 \sin^2 \frac{T}{2} \bar{\omega}$$

and

$$\epsilon_{tot} = 2 \sum_{m=1}^{10} \epsilon$$

for time shifts alone.

And considering both time and frequency shifts

$$\epsilon_{tot} \simeq \sum_{m=1}^{10} \epsilon$$

$$\simeq 4 \sum_{m=1}^{10} \sin^2 \frac{T}{2} \bar{\omega}$$

where

$$T_n \simeq 3.9 \times 10^{-4} \sum_{m=1}^{n} m$$

$$\epsilon_{tot} \simeq 5.5 \times 10^{-3}$$

$$\text{rms error} \simeq \sqrt{\epsilon_{tot}}$$

$$\simeq 0.08$$

Hence, the minimum error (in the worse case between -5 HA and +3 HA), using the assumption of constant frequency, is approximately 8 percent. Although this is above the error for which the approximations are reasonable, the order of magnitude of the error is obtained. This indicates that, in the worse case, we should not assume constant frequency fringes, but should proceed as in Appendix IV.

APPENDIX IV

TO OBTAIN THE FRINGE PATTERN WHEN THE FRINGE FREQUENCY VARIES APPRECIABLY

(a) General

Let the computer calculate the period of each fringe and the sidereal time at the beginning (or center) of each fringe cycle in terms of the sidereal time at the beginning of the whole interferometer scan (which is recorded on tape). If ten samples* per second are taken, and the first cycle period is very slightly less than one second, then there is a phase difference between the first point in the first cycle and the first point in the second: similarly, with other "corresponding" points in the first two cycles, and in all cycles. Hence, all points in a cycle may be given their correct phase (relative to the start of the first cycle). All points are grouped in equal phase intervals over the cycle, and the average of each group taken. Thus, we have one cycle of fringe sine wave which contains all observations, where the commencement of the one cycle corresponds to many sidereal times.

Two important advantages emerge from this treatment:

i. Provided the computer program gives the period of each fringe, and the phase of each point in its own cycle, then a single cycle of the fringe pattern is produced; each point on the sine wave now has a smaller standard deviation.

ii. Longer scan times may be used, giving an effective increase in integration time.

The computation required for this method is only a little more complex than that required for the fixed frequency case in Appendix II, and the solution for Θ and A (in Appendix V) is the same. In fact, since longer scans are possible the increased integration time may be long enough to permit the amplitude and phase of all but smallest fringes to be determined by simple interpolation methods. The chief limitation to the extension of integration time is the "smearing" of the observation point of the Fourier transform diagram (u-v diagram).

---

* This is not strictly sampling, although the term is useful. The "sampling" rate is determined by the minimum number of samples permissible in the fastest fringe period (see Appendix V).

(b) Program Outline — To Obtain a Sine Wave Where Fringe Frequency Varies

Consider interferometer fringes of varying frequency, the period of each individual cycle being computed (which may be done using the sidereal time of the cycle commencement — or its approximate mid-point, as is preferred). Assuming a constant rate of sampling, during which period pre-integration occurs, we may use the following digital computer program outline to obtain the single fringe cycle described in the previous section of this Appendix. We assume ten points are required to plot the sine wave, i.e., we have ten (equal) phase-intervals.

Referring to Figure XI, we define the following terms:

t = sampling interval and pre-integration time (a constant)

T_i = period of i^{th} fringe

$\frac{t}{T_i}$ = portion of cycle per sample

m = an integer

Θ_i = "remnant" time

S = sidereal time at beginning of scan (first sample)

a = number of equal intervals into which one cycle is split (here $a = 10$)

X_k = sum of all R's in k^{th} interval

Z_k = number of R's in k^{th} interval

Program Outline

Store S

Store t

Clear storage for X_1, $X_2 \ldots X_{10}$ and registers for Z_1, $Z_2 \ldots Z_{10}$

$i = 0$

$S_i = S$

$\Theta = -t$

(1) $\Theta = H$

$i = i + 1$

Compute T_i (program already exists)

$$P = \frac{t}{T_i}$$

$$R = \frac{t - \Theta}{T_i}$$

(2) → W = tape sample

Move on tape to next sample

$R = R + P$

If $R \leq 0.1$ ($R \neq 0$)

If $R > 0.1$

$X_1 = X_1 + W$

To (3) ← $Z_1 = Z_1 + 1$

If $R \leq 0.2$

If $R > 0.2$

$X_2 = X_2 + W$

To (3) ← $Z_2 = Z_2 + 1$

If $R \leq 0.3$

. . . . . .

. . . . . .

If $R \leq 0.9$

If $R > 0.9$

$X_9 = X_9 + W$

To (3) ← $Z_9 = Z_9 + 1$

$X_{10} = X_{10} + W$

$Z_{10} = Z_{10} + 1$

(3) → Look for "end of scan" marker

To (4) ← If affirmative

If negative, continue

$Q = 1 - R$

$M = Q - P$

To (2) ← If $M \geq 1$

If $M < 1$, continue

$H = Q$

Print S_i with corresponding i

To (1) ← $S_i = S_i + T_i$

(4) → $Y_1 = \frac{X_1}{Z_1}$ Print

$Y_2 = \frac{X_2}{Z_2}$ Print

.....

.....

$Y_{10} = \frac{X_{10}}{Z_{10}}$ Print

End of Program

APPENDIX V

THE NUMBER OF POINTS TO DEFINE AMPLITUDE AND PHASE OF A SINE WAVE

(a) Minimum Number of Integrations Per Cycle

Consider the maximum error in integrating a portion of a sine wave. This will occur at the peak of the sine wave. Let the integrating time be 2h. Thus, the error in integrating the shaded portion (Figure XII) is

$$\epsilon = \frac{1}{2h} \int_{X_o - h}^{X_o + h} \cos X \, dX \quad - \cos X_o$$

Hence

$$\epsilon = \frac{\sin h}{h} - 1 \cos X_o \quad - (1)$$

And when $X_o = n\pi$ (maximum error)

$$\epsilon = \frac{h - \frac{h^3}{6} + \frac{h^5}{120} - \ldots}{h} - 1$$

$$= -\frac{h^2}{6} \text{ for small h}$$

For 10 points per cycle $h = 18^\circ \simeq 0.3$ radians

$$\epsilon = -1.5 \text{ percent}$$

Apart from the fact that this is the maximum error, and only occurs for the highest fringe frequency (assuming constant sampling rate), the correction to each point on the sine wave may be calculated from (1).

(b) To Determine The Amplitude and Phase of One Cycle of Sine Wave, Using the Method of Least Squares Fit.

The cycle period is known, and is split into an equal number of intervals (see Figure XIII). The observed points have the form

$$y_i = A \sin (z_i - \Theta) + \epsilon_i$$

where ϵ_i is a normally distributed error, representing the noise-to-signal ratio

$$A = \text{amplitude}$$

$$\Theta = \text{phase}$$

$$S = \sum_{i=10}^{n} [A \sin (z_i - \Theta) - y_i]^2$$

For S = minimum, we get (after some reductions):

$$A [U \cos^2 \Theta - 2V \cos \Theta \sin \Theta + W \sin^2 \Theta] = X \cos \Theta - Y \sin \Theta$$

$$A [V \cos^2 \Theta + (U - W) \cos \Theta \sin \Theta - V \sin^2 \Theta] = Y \cos \Theta + X \sin \Theta$$

where

$$U = \sum_{i=1}^{n} \sin^2 z_i \qquad V = \sum_{i} \sin z_i \cos z_i$$

$$W = \sum_{i} \cos^2 z_i \qquad X = \sum_{i} y_i \sin z_i$$

$$Y = \sum_{i} y_i \cos z_i$$

Thus we have the third-order equation in tan Θ:

$$\frac{U - 2V \tan \Theta + W \tan^2 \Theta}{V + (U - W) \tan \Theta - V \tan^2 \Theta} = \frac{X - Y \tan \Theta}{Y + X \tan \Theta}$$

A computer program has been devised for solving this cubic, and proceeds as follows:

Let the cubic be F (tan Θ) = 0

Compute S(Θ) for 0°, 60°, 120°, 180°, 240°, 300°

Choose the value of Θ giving the smallest value of S. This is our "first guess" in the solution of the cubic.

Take a value of Θ about 10° above the first guess (call this point "second value") and determine where the chord through these two points crosses the line $F(\tan \Theta) = 0$ (see Figure XIV). Let this value of $\tan \Theta$ be the "third value", and let it replace "first guess" in determining where the chord through "second value" and "third value" crosses the line $F(\tan \Theta) = \Theta$. Thus, we get "fourth value" (which replaces "second value"), etc. This method converges very rapidly to the required solution, so only a few iterations are required. The other solutions to the cubic may now be obtained by substituting the first solution and solving the quadratic. These two solutions for $\tan \Theta$ should be less significant than the first, since they should be imaginary or complex. (Trials on the computer have to date produced the significant solution first in all cases.)

Since the significant solution is for $\tan \Theta$, and since Θ lies between 0 and 2π, identical solutions for $\tan \Theta$ occur for Θ and $\Theta + \pi$. Thus, we must obtain $S(\Theta)$ and $S(\Theta + \pi)$ and take the smallest. This gives the value of Θ that is substituted back in order to obtain A.

(c) To Determine the Accuracy of Θ and A.

After pre-integration, a second integration occurs when samples in a given "phase interval" (see Appendix IV) are averaged. Hence

$$\sigma = \frac{\text{Noise}}{\text{Signal}} = \frac{T_s}{2T_A} \cdot \frac{1}{\sqrt{B\tau m}}$$

$$\tau = \frac{t}{n}$$

where n = number of samples per cycle, and t = cycle period. Thus

$$\sigma = \frac{T_s}{2T_A} \cdot \sqrt{\frac{n}{Btm}}$$

Since the product t x m is constant for a given total integration time, fringe period variation does not affect σ. The minimum fringe period is 0.7 seconds, B = 8 Mc, T_s = 1000 °K, and T_A = 1 °K ($S \simeq 0.6$ flux units for two 85-foot dishes), and

$$\sigma \simeq 0.2 \sqrt{\frac{n}{m}}$$

This is identical to $T_s = 150\ ^\circ K$ and $T_A = 0.15\ ^\circ K$.

For von Hoerner's criterion [13] to be rigorously fulfilled $m \geq n$. A more useful form is

$$\sigma \simeq 0.02\sqrt{n}$$

for a one minute scan. The value of σ is determined, and given to a gaussian random number generator in order to simulate noise on sine waves of varying phase. A computer program then determines the errors in Θ and A from many solutions of the cubic (discussed in the preceding section of this Appendix). This is repeated for many values of n, so that σ_A and σ_Θ may be plotted against n. These results will be available shortly.

APPENDIX VI

THE USEFUL PRECISION OF THE DIGITAL RECORD

Let the number of contributions to each point on a single sine wave (Appendices IV and V) be fairly large (> 20, say). Then according to Vinokur [17] the fractional rms noise increase (i.e., fractional increase in standard deviation) is

$$\Delta\sigma = \frac{1}{24\alpha^2}$$

where α is the number of digits corresponding to a minimum temperature, T_{min}. If the equivalent fringe amplitude temperature, T_A, is small compared with the system noise temperature, T_s, then $\Delta\sigma$ is effectively constant for all T_A. Hence, $\Delta\sigma$ and T_{min} are determined, and α is obtained.

For crystal mixers

$$\sigma = \frac{0.02}{T_A}\sqrt{n}$$

From von Hoerner's criterion, for n = 10

$$T_A = T_{min}$$

$$= 0.3\ ^\circ K$$

A one percent error in standard deviation gives

$$0.01 = \frac{1}{24\alpha^2}$$

$$\alpha = 2 \text{ digits per } T_{min}$$

$$\text{i.e., } T_D = 0.15\ ^\circ K$$

$$\text{where } \alpha = \frac{T_{min}}{T_D}$$

For parametric amplifiers, von Hoerner's criterion gives

$$T_{min} = 0.05\ ^\circ K$$

and a one percent error in σ requires

$$T_D = 0.025\ ^\circ K$$

An important point, when considering the number of digits required, is the dynamic range of the digital equipment. Figures III and VIII show that the maximum signal which will be received from Cygnus A on the NRAO inteferometer is below one hundredth of the maximum fringe amplitude. This situation appears to occur with most of the strong sources, since these are well resolved at the shortest NRAO baseline. Hence, most of the strongest sources will give maximum fringe amplitudes representing antenna temperatures $< 10\ ^\circ K$. This gives a much smaller dynamic range than would at first appear, and three decimal digits (three lines on the tape) will give a range of $-12.5\ ^\circ K$ to $+12.5\ ^\circ K$ (since the correlation interferometer gives positive and negative output signals) in steps of $0.025\ ^\circ K$. Only two tape lines would be required in this case if binary code was used.

APPENDIX VII

THE POINT SOURCES

From Conway, Kellerman and Long [14], the point sources with estimated flux > 0.6 flux units are listed below. For our purposes a point source is a source which was unresolved by Jodrell Bank at 32,000 λ and 158 Mc [2].

The sources 3C 49, 3C 85 and 3C 222 are not in the catalog of Conway, Kellerman and Long, so a considerable extrapolation was required from the Jodrell Bank data, assuming $\alpha = 0.7$. The sources 3C 119, 3C 299, and 3C 459 appear in Conway, Kellerman and Long and require considerably less extrapolation, while the remaining three source fluxes are given directly.

Source	δ	$S_{10\ cm}$	T_A
3C 48	+33°	8.4 flux units	3.4 °K
3C 49	+13°	1.2 flux units	0.5 °K
3C 85	+17°	1.0 flux units	0.4 °K
3C 119	+41°	4.5 flux units	1.8 °K
3C 147	+50°	11.4 flux units	4.6 °K
3C 222	+5°	1.5 flux units	0.6 °K
3C 286	+31°	9.5 flux units	3.8 °K
3C 299	+42°	1.5 flux units	0.6 °K
3C 459	+4°	2.5 flux units	1.0 °K

REFERENCES

[1] "Accurate Measurement of the Declinations of Radio Sources," R. B. Read. Ap. J., 138, 1, p. 1 (1963).

[2] "An Analysis of the Angular Sizes of Radio Sources," Allen, Hanbury Brown, Palmer. Mon. Not. R.A.S., 125, 1, p. 57 (1962).

[3] "Brightness Distribution of Discrete Radio Sources," P. Maltby and A. T. Moffet. Ap. J. Suppl., 7, p. 93 (1962).

[4] "Mesures Inteférométriques à Haute Résolution du Diamètre et de la Structure des Principales Radiosources a 1420 MHz," J. Lequeux. Annales d' Astrophysique, 25, 4, p. 221 (1962).

[5] "High Resolution Observations with a Radio Tracking Interferometer," B. Rowson. Mon. Nat. R.A.S., 125, 2, p. 177 (1963).

[6] "The Potentialities and Present Status of Masers and Parametric Amplifiers in Radio Astronomy," J. V. Jelley. P.I.E.E.E., 51, 1, p. 30 (1963).

[7] Personal communication - P. G. Mezger.

[8] "Sensibilité des Radiotélescopes et Récepteur a Corrélation," E. J. Blum. Annales d' Astrophysique, 22, 2, p. 139 (1959). English translation at NRAO.

[9] "A Calculation of the Fringe Pattern for a Correlation Interferometer," W. R. Burns. N.R.A.O. Internal Report (1963).

[10] "Limitations on the Accuracy of Angular Location of a Radio Star Using Interferometer Techniques," L. S. Wagner. Cornell University Research Report EE 378 (1958).

[11] "Statistical Theory of Communication," Y. W. Lee. (J. Wiley) Chapter 12.

[12] "A Digital Spectral Analysis Technique and Its Applications to Radio-Astronomy," S. Weinreb. PhD Thesis, M.I.T. (1963).

[13] "Very Large Antennas for the Cosmological Problem: I. Basic Considerations," S. von Hoerner. N.R.A.O. Pub. 1, 2 (1961).

[14] "The Radio Frequency Spectra of Discrete Radio Sources," Conway, Kellerman, Long. Mon. Not. R.A.S., 125, 3 and 4, p. 261 (1963).

[15] "Observations of the Crab Nebula With the Pulkovo Radio Telescope" (λ = 3 cm), Apushkinskii and Pariiskii. Sov. Ast., 3, p. 717 (1959).

[16] "Integration of a DC Signal Mixed With Noise: Filtering and Useful Rate of Sampling," M. Vinokur. N.R.A.O. Internal Memorandum (1961). Numerical corrections to above - Vinokur and Keen, N.R.A.O. (1963).

[17] "Useful Precision for the Measurement of a Signal Mixed With Noise," M. Vinokur. N.R.A.O. Internal Memorandum (1961).

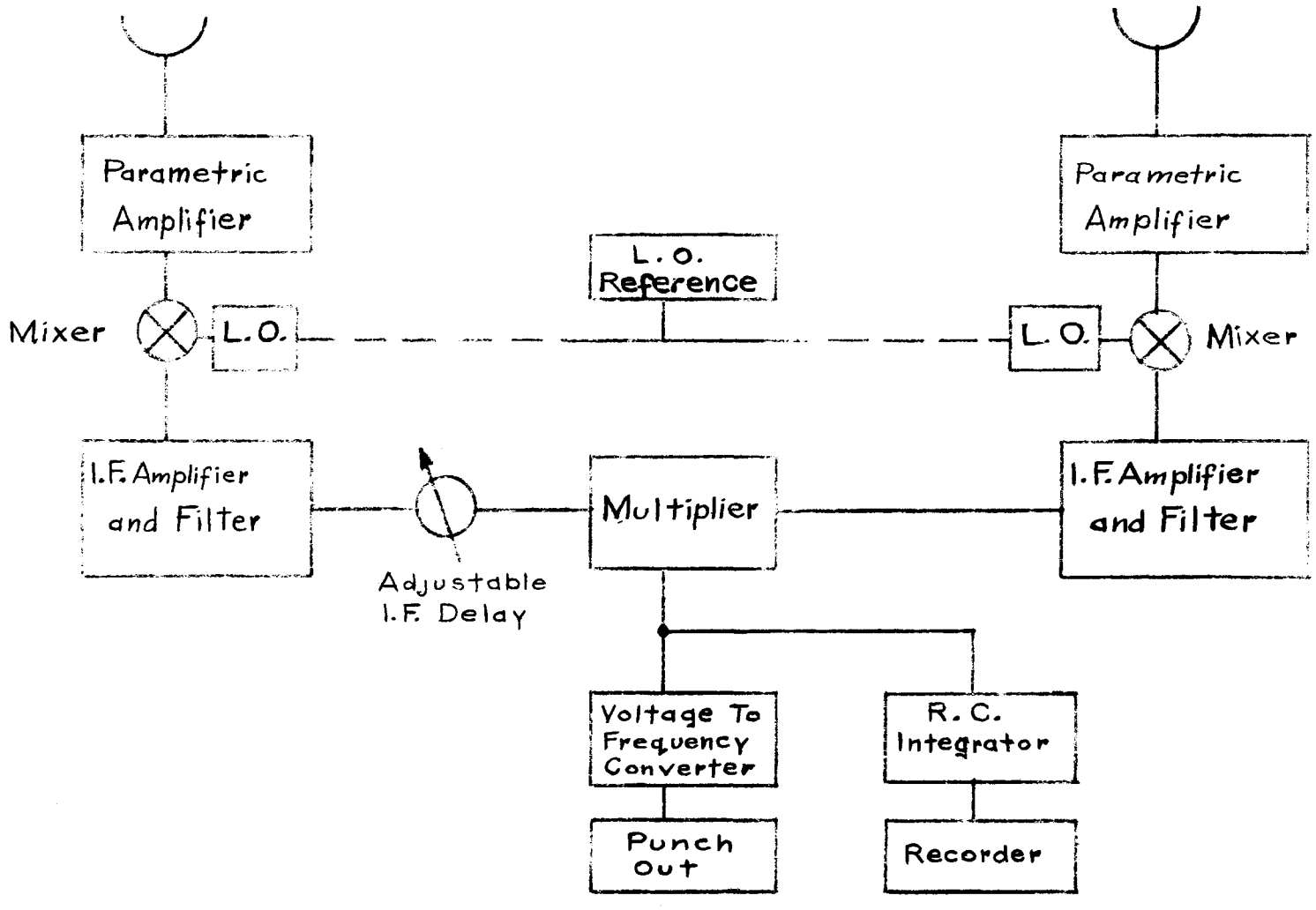

THE N.R.A.O. INTERFEROMETER SYSTEM

FIG. I (a)

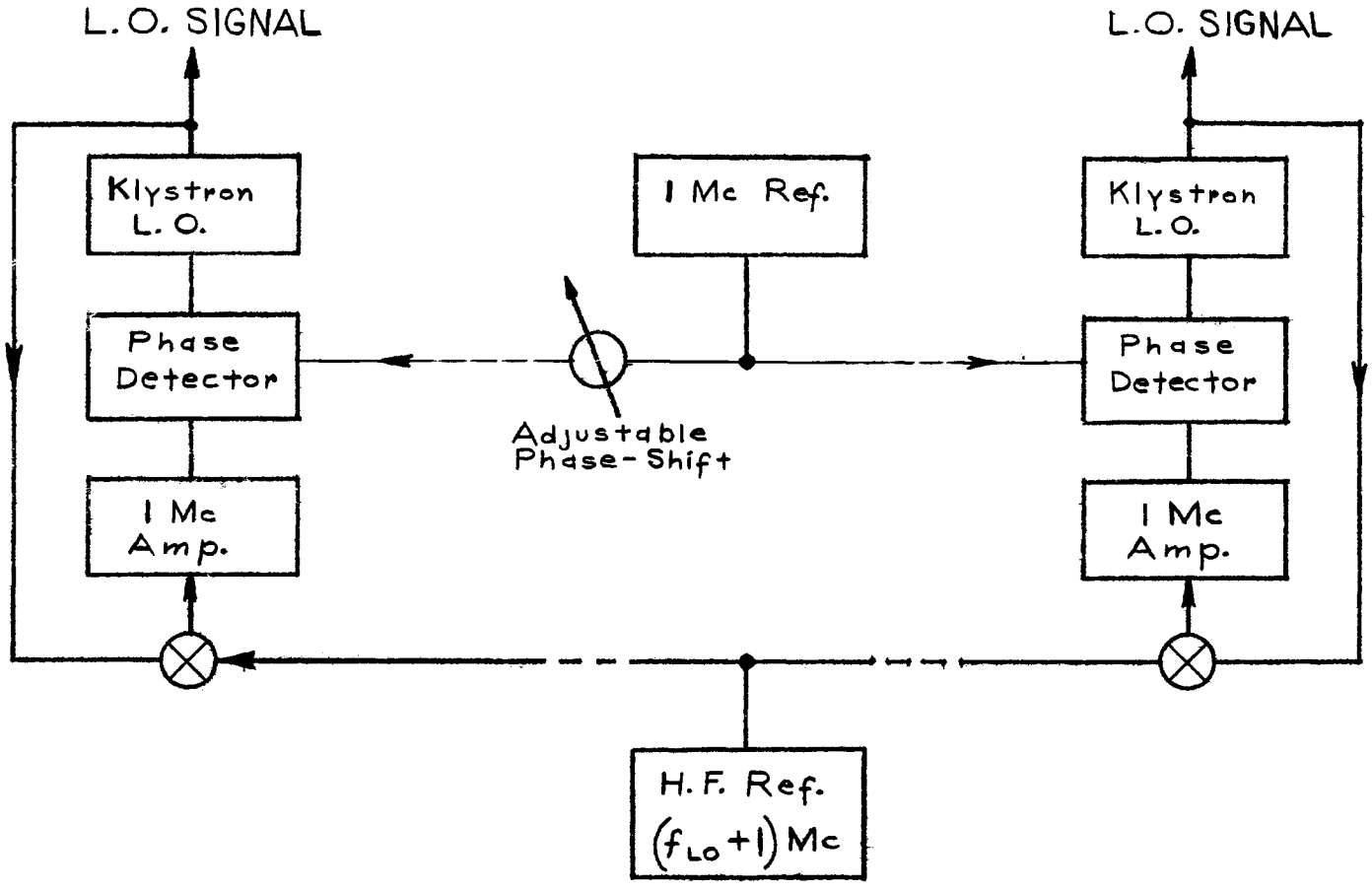

THE PHASE LOCK SYSTEM

FIG. I(b)

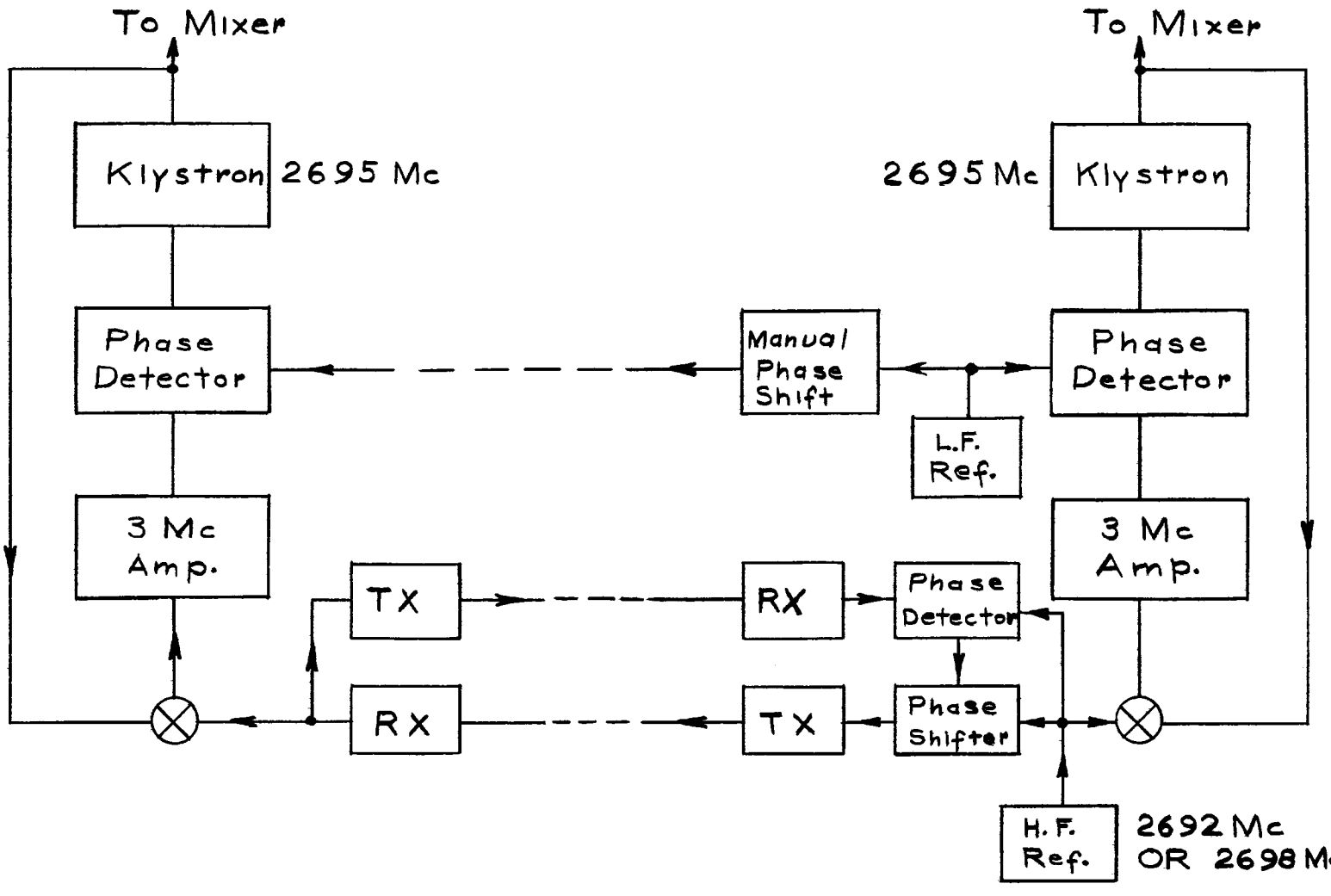

MODIFIED PHASE-LOCK SYSTEM

FIG. I(c.)

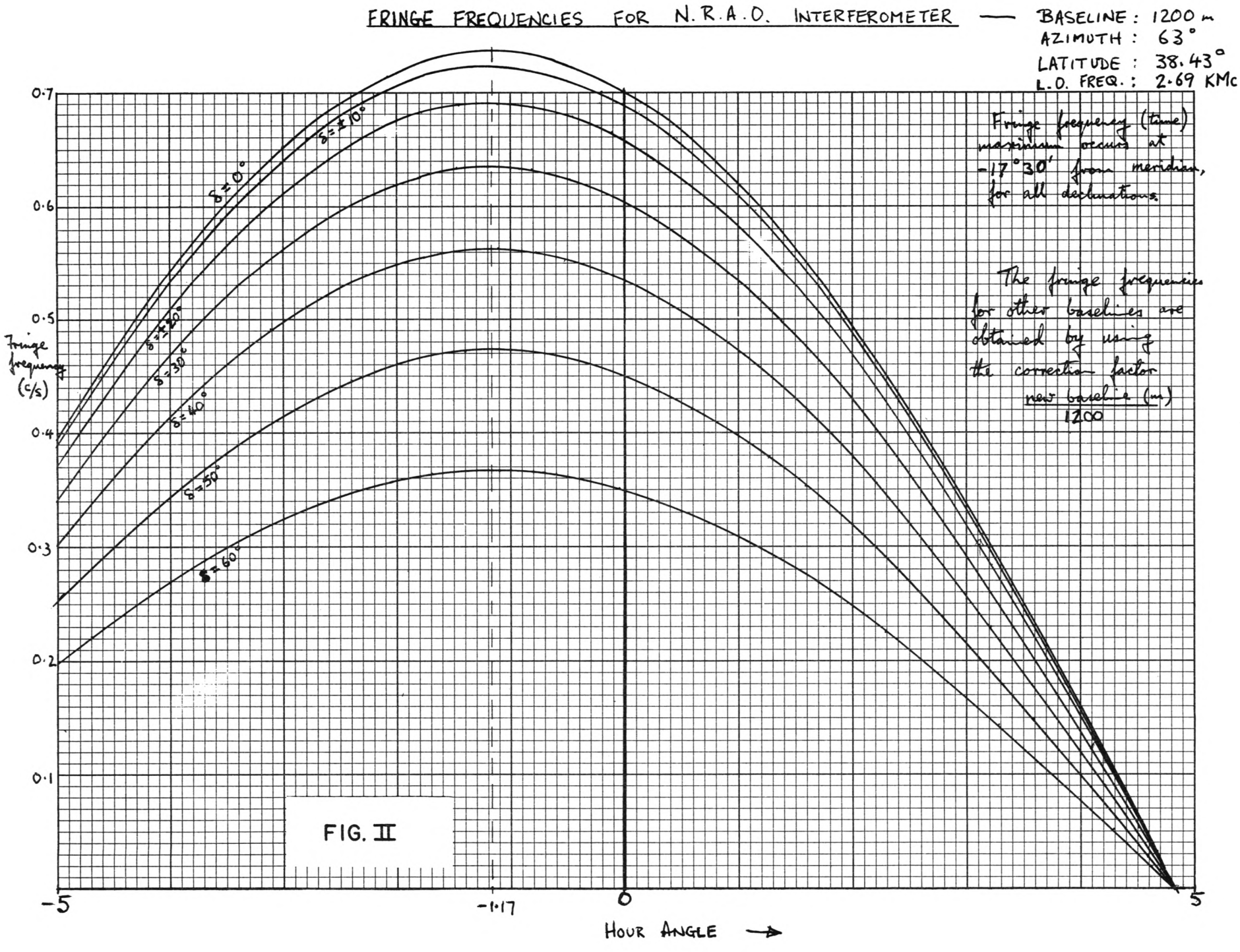
FRINGE FREQUENCIES FOR N.R.A.O. INTERFEROMETER
BASELINE : 1200 m
AZIMUTH : 63°
LATITUDE : 38.43°
L.O. FREQ. : 2.69 KMc
Fringe frequency (time) maximum occurs at -17°30' from meridian, for all declinations.
The fringe frequencies for other baselines are obtained by using the correction factor
new baseline (m) / 1200
δ = 0°
δ = ±10°
δ = ±20°
δ = 30°
δ = 40°
δ = 50°
δ = 60°
Fringe frequency (c/s)
0.7
0.6
0.5
0.4
0.3
0.2
0.1
-5
-1.17
0
5
HOUR ANGLE →
FIG. II

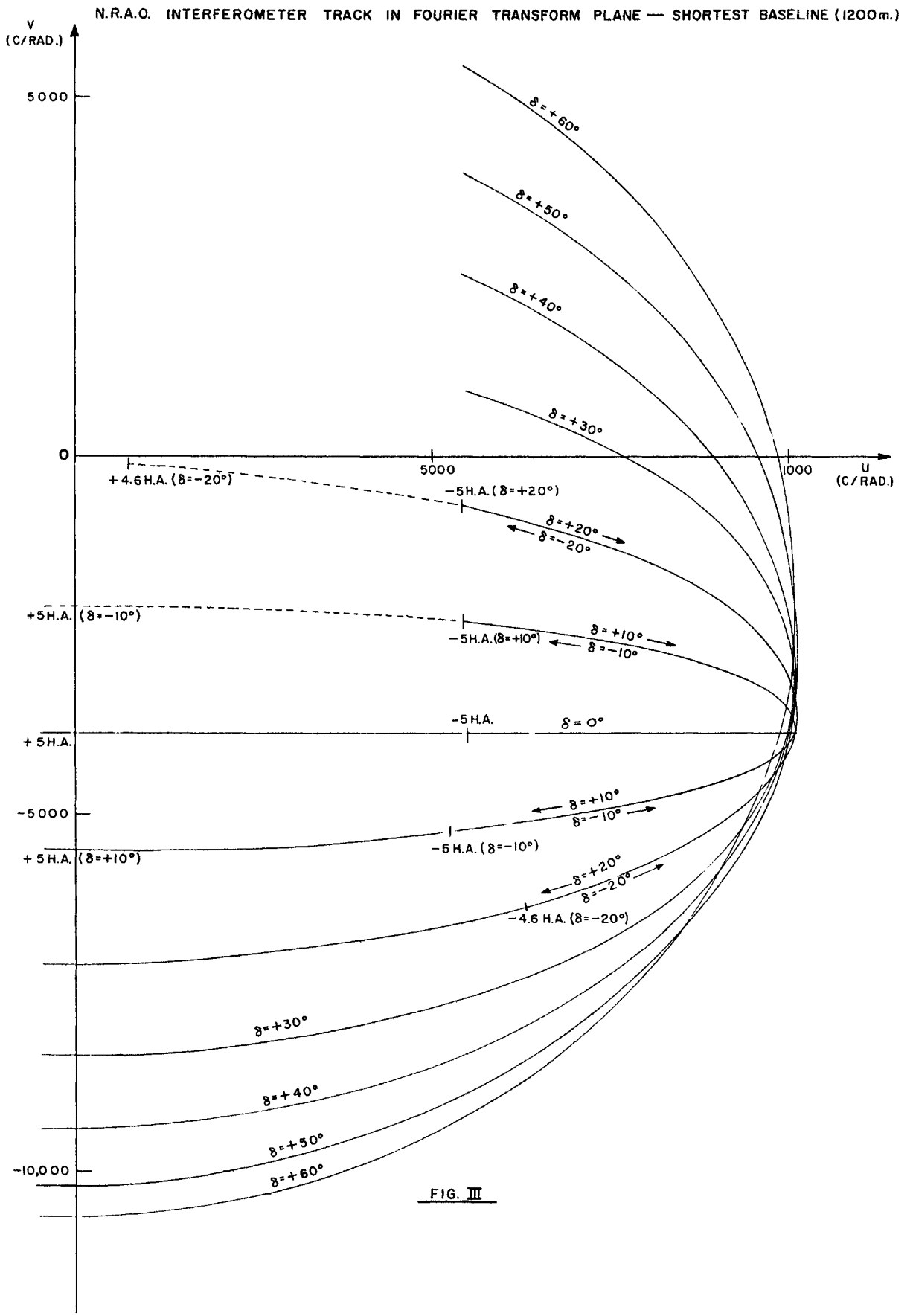
N.R.A.O. INTERFEROMETER TRACK IN FOURIER TRANSFORM PLANE — SHORTEST BASELINE (1200m.)
V (C/RAD.)
5000
0
-5000
-10,000
U (C/RAD.)
5000
1000
δ = +60°
δ = +50°
δ = +40°
δ = +30°
+4.6 H.A. (δ = -20°)
-5 H.A. (δ = +20°)
δ = +20°
δ = -20°
+5 H.A. (δ = -10°)
-5 H.A. (δ = +10°)
δ = +10°
δ = -10°
-5 H.A.
δ = 0°
+5 H.A.
δ = +10°
δ = -10°
-5 H.A. (δ = -10°)
+5 H.A. (δ = +10°)
δ = +20°
δ = -20°
-4.6 H.A. (δ = -20°)
δ = +30°
δ = +40°
δ = +50°
δ = +60°

FIG. III

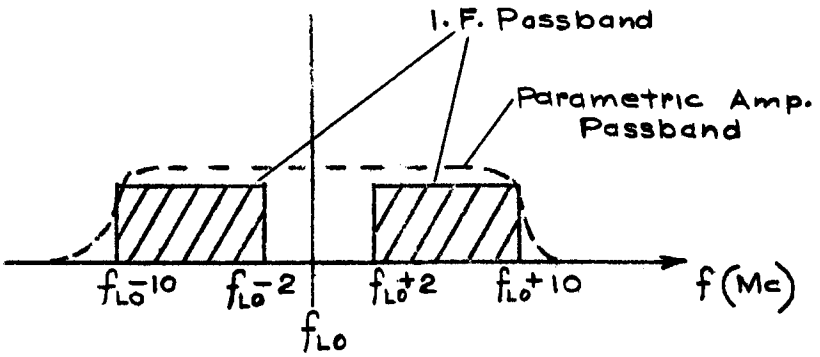

FIG. IV

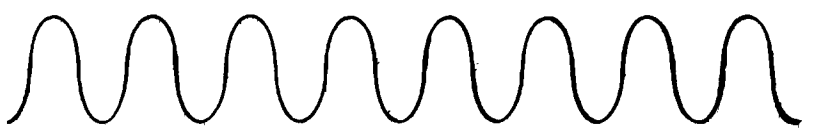

Interferometer Fringes

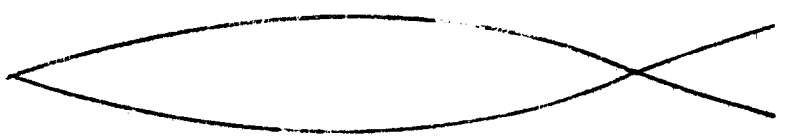

Cosine Envelope

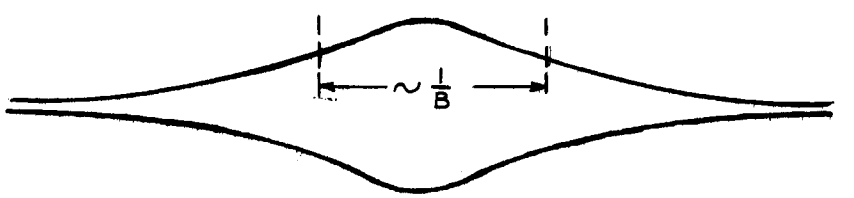

Passband Modulation

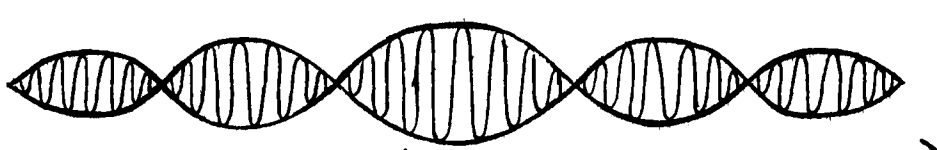

Resultant Fringe Pattern (With Contracted Time Scale)

FIG. V

(Curves Not To Scale)

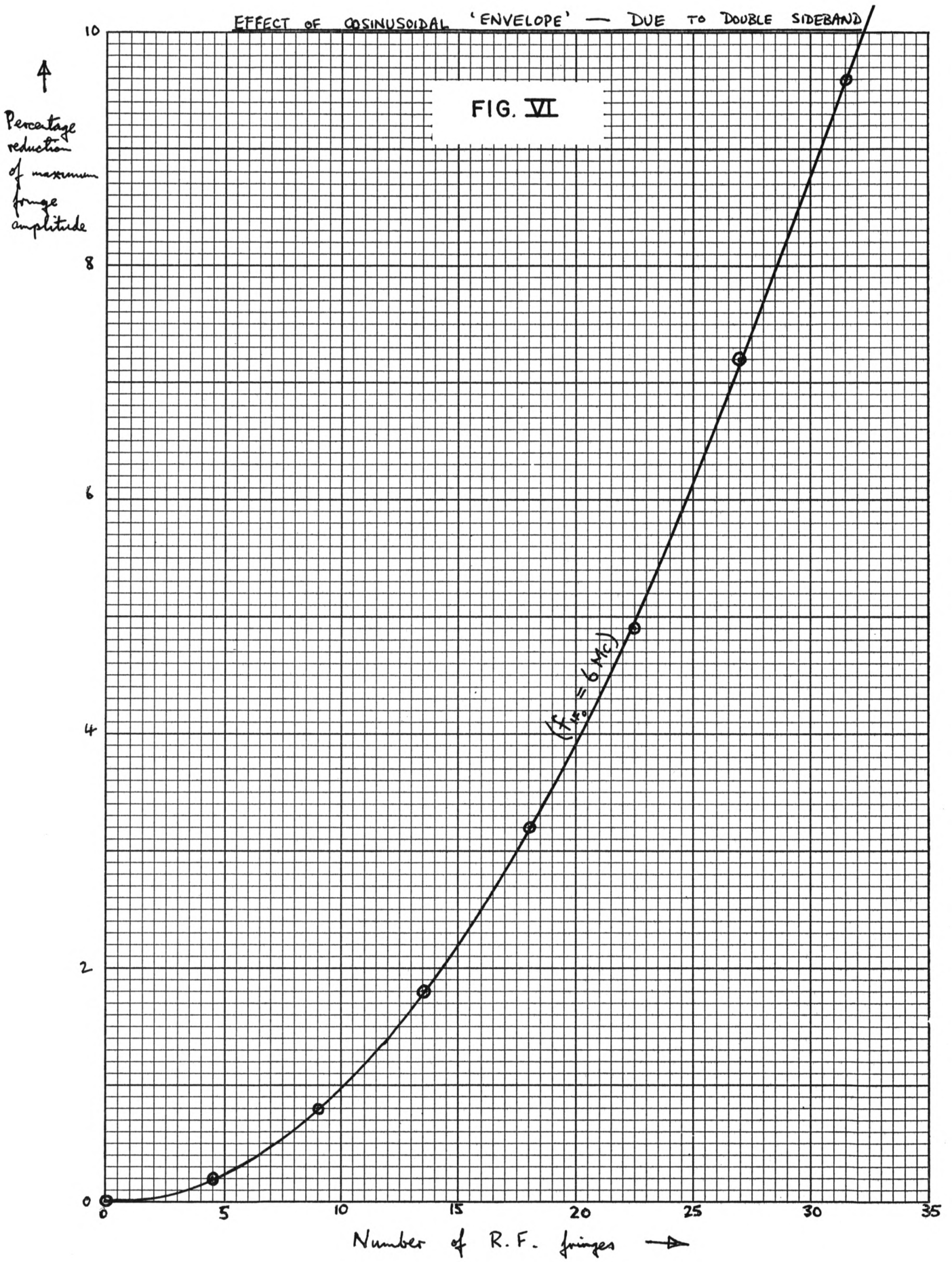
EFFECT OF COSINUSOIDAL 'ENVELOPE' — DUE TO DOUBLE SIDEBAND
FIG. VI
Percentage reduction of maximum fringe amplitude
10
8
6
4
2
0
0
5
10
15
20
25
30
35
Number of R.F. fringes
(f_x = 6 Mc)

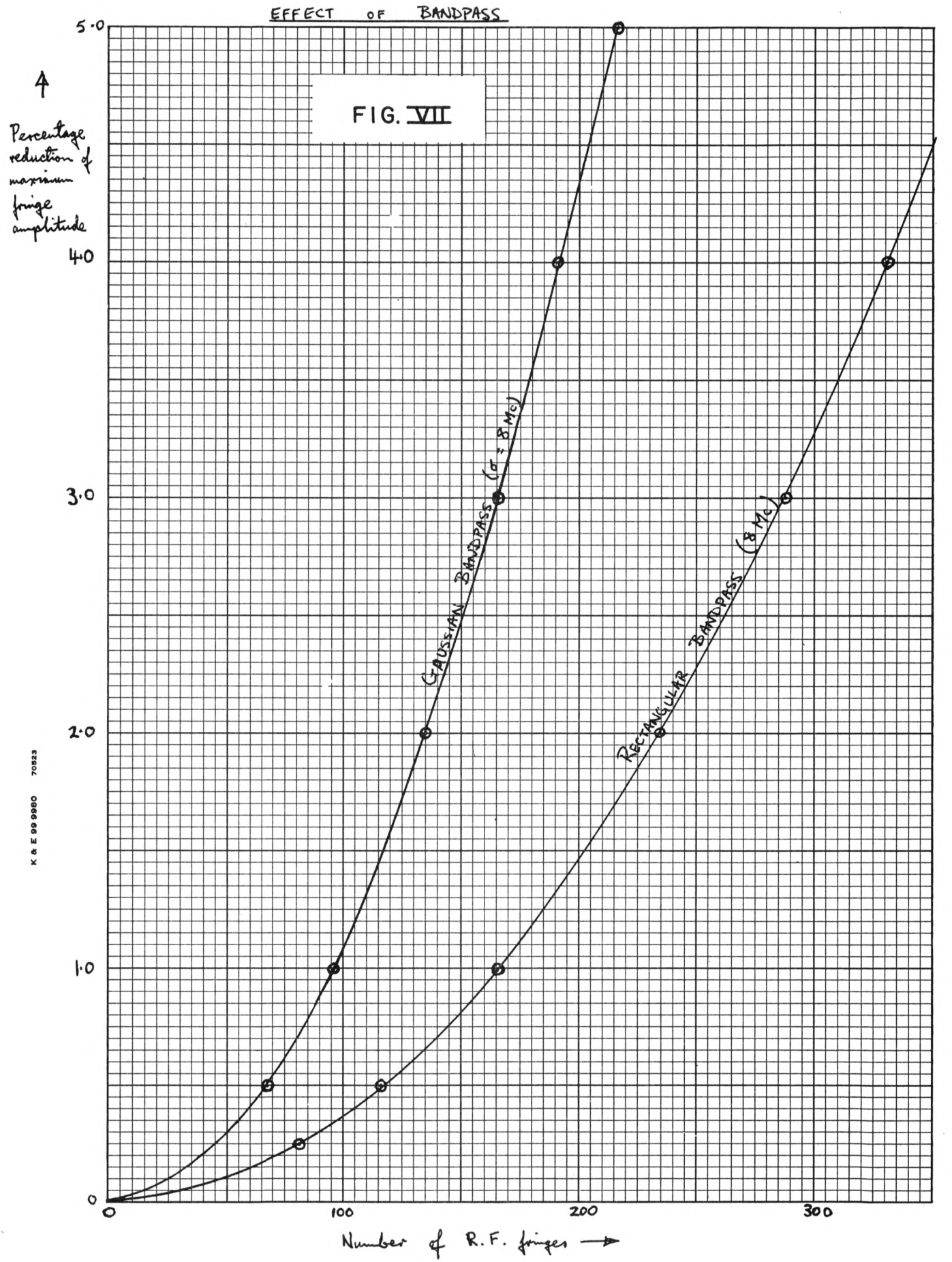
EFFECT OF BANDPASS
FIG. VII
4
Percentage reduction of maximum fringe amplitude
5·0
4·0
3·0
2·0
1·0
0
0
100
200
300
Number of R.F. fringes →
GAUSSIAN BANDPASS (σ = 8 Mc)
RECTANGULAR BANDPASS (8 Mc)
K & E 99 9980 70523

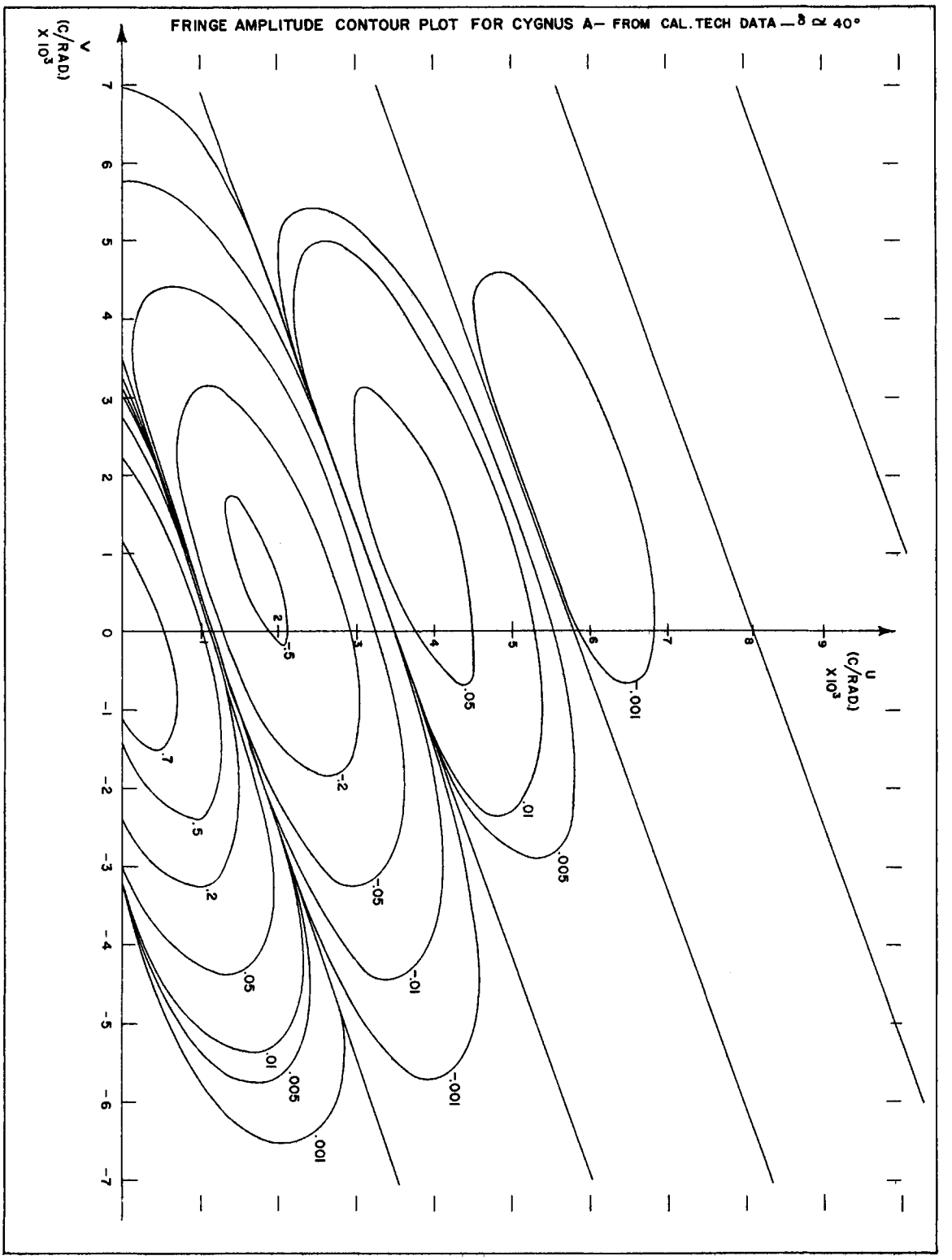
FRINGE AMPLITUDE CONTOUR PLOT FOR CYGNUS A— FROM CAL. TECH DATA — δ ≅ 40°
V (C/RAD.) X 10³
U (C/RAD.) X 10³
7
6
5
4
3
2
1
0
-1
-2
-3
-4
-5
-6
-7
-9
-8
.7
.5
.2
.05
.01
.005
.001
-.5
-.2
-.05
-.01
-.001

FIG. VIII

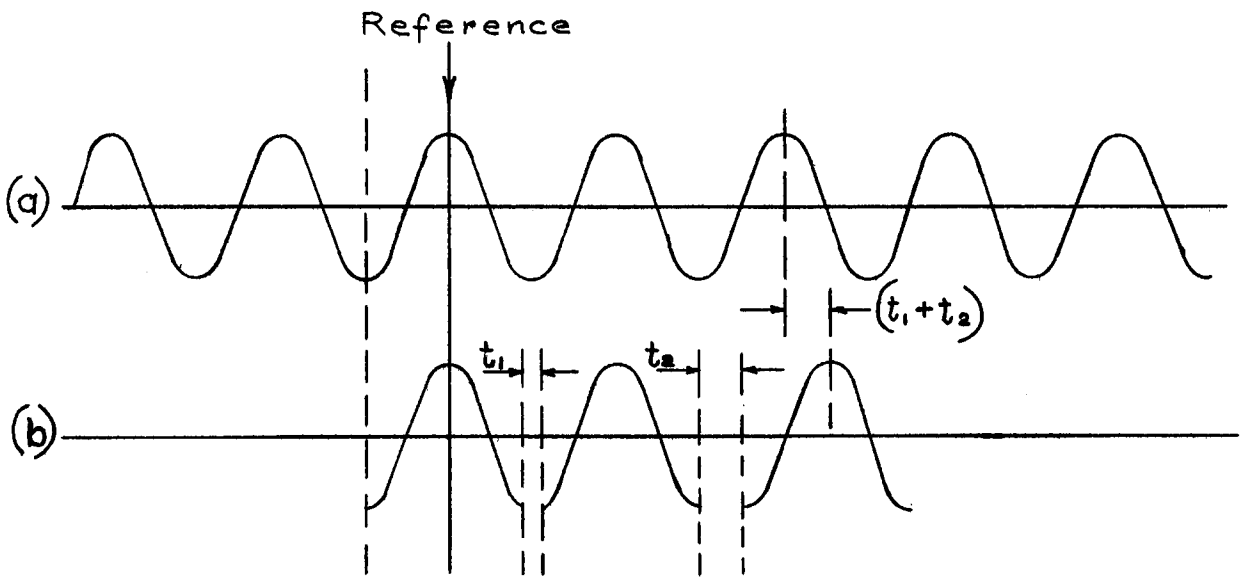

FIG. IX

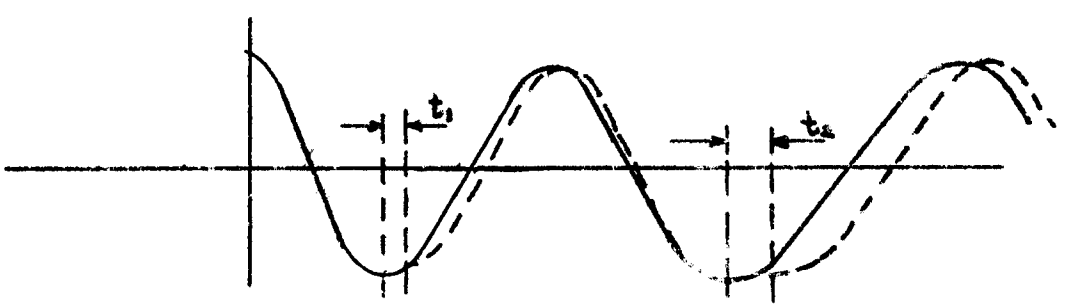

FIG. X

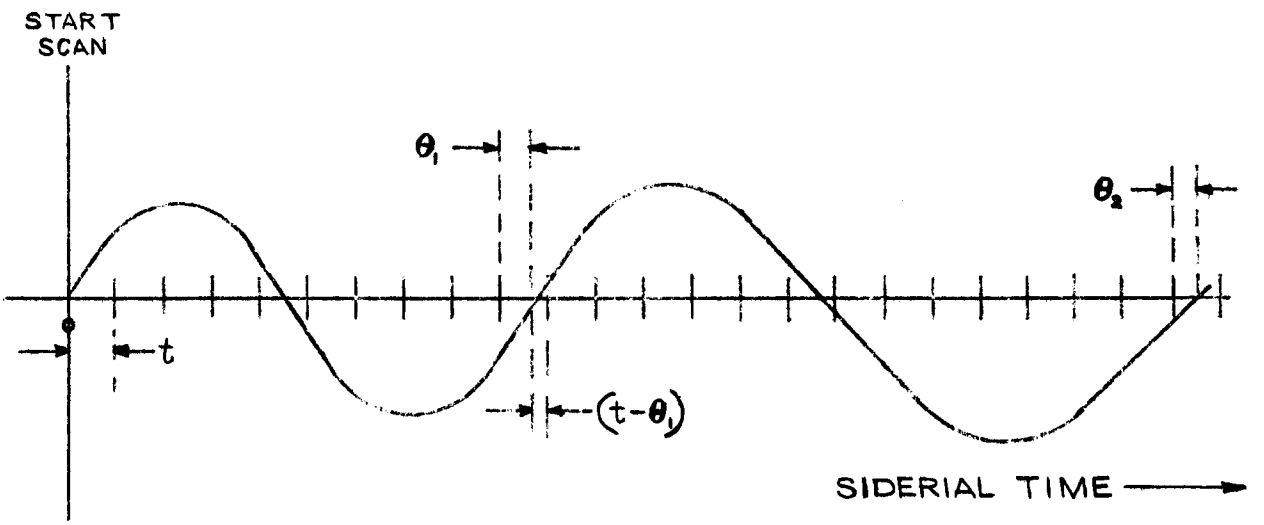

FIG. XI

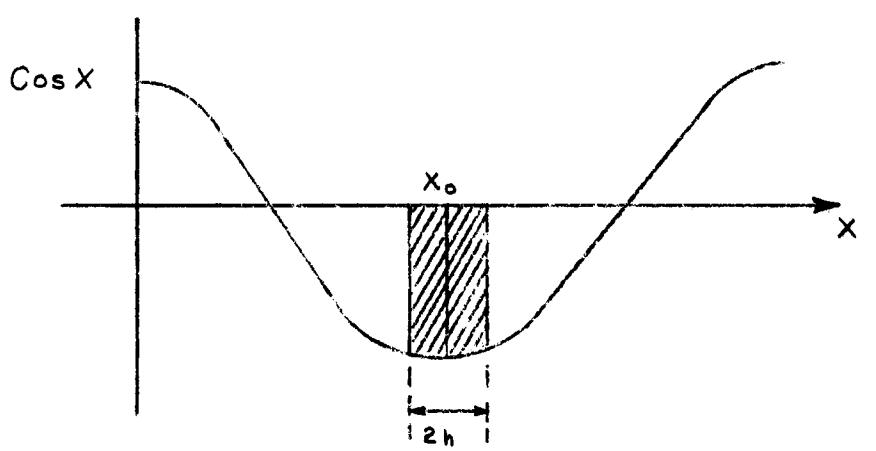

FIG. XII

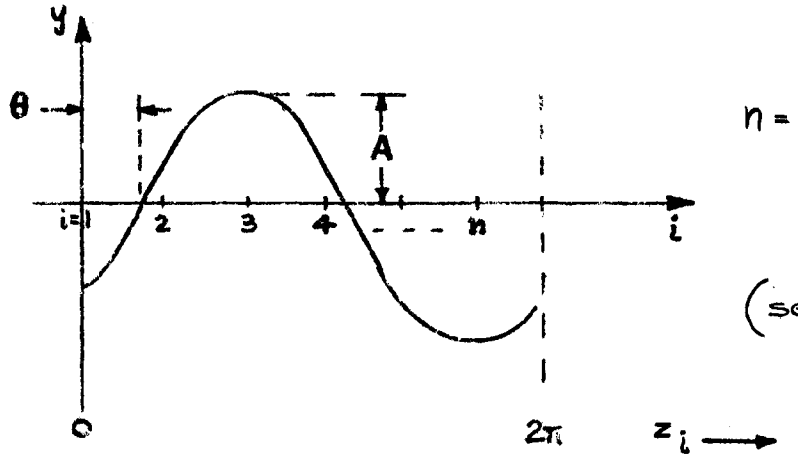

FIG. XIII

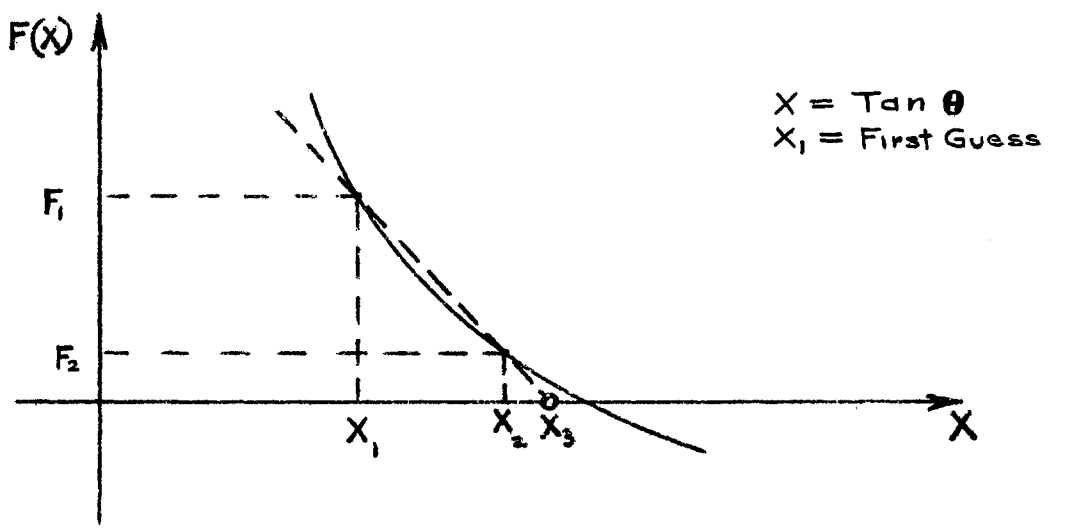

FIG. XIV